Constitutive Parameters Identification of AZ31B-H24 Magnesium Alloy and Energy-Absorption Analysis in Structural Panel Use

Yuedong Yang[1,2], Jiqing Chen[1,2], Fengchong Lan[1,2], Wu Zeng[3] and Zhengwei Ma[4]

[1]*School of Mechanical & Automotive Engineering, South China University of Technology, Guangzhou, 510641, China*
[2]*Guangdong Province Key Laboratory of Automotive Engineering, Guangzhou, 510641, China*
[3]*School of Mechanical Engineering, Beijing Institute of Technology, Beijing, 100081, China*
[4]*College of Mechatronics and Control Engineering, Shenzhen University, Shenzhen, 518060, China*

Abstract. As a novel lightweight material, AZ31B magnesium alloy is considered as the most potential material to instead baseline steel in some automotive parts. However, their structural use is quite limited and so far proper numerical modeling has not been developed to represent magnesium alloy. In present study, the Split Hopkinson Pressure Bar (SHPB) test is utilized to investigate material dynamic mechanism for AZ31B-H24 over a wide range of strain rates from 1389 s^{-1} to 7296 s^{-1}. Parametric identification for Johnson-Cook (J-C) constitutive model available in the commercial finite element package LS-DYNA is carried out. Proper parameters are obtained by curve fit using genetic algorithm with experimental results. Constitutive model after parametric identification is applied to automotive outer panels for crashworthiness analysis. Energy absorption with magnesium alloy substituted baseline steel under lightweight 51.18% is obtained and the key problem of thin-walled magnesium alloy applied in automotive structure is advanced.

1 Introduction

Stricter regulations on fuel economy and growing concerns on automotive emissions have led to an increased focus on vehicle weight reduction [1]. Automotive lightweight is considered as key strategy to improve fuel consumption and reduce artificial environmental damage emissions [2, 3]. Application of lightweight materials is regard as the most effective way to reduce weight. Magnesium alloys are ideal candidate materials in comparison to baseline steel or aluminum alloys due to their low density, high strength-to-weight ratio, good durability, recyclable, excellent fatigue, potential reduction in part count due to larger castings and the ability of improving structural NVH (Noise, Vibration and Harshness) [4-8]. However, structural use of magnesium alloys is very limited, and even proper material numerical modeling have not been developed to establish crash models as well as forming processes. As we all know, the stress, strain and strain rate of magnesium alloy materials will be changed over the crash and forming process in automotive industry. It always covers high strain rate in these dynamic process. But little knowledge of their dynamic mechanism for magnesium alloys is available [9].

When the dynamic processes with large deformation, highly nonlinear characteristics such as crashworthiness, punch forming and so on are occurred, the constitutive relationships of materials are changed obviously, which result in strain hardening, rate-dependent and thermal softening [10]. Proper material constitutive parameter is the key to connect simulations with experiments. It's an important step to determine the constitutive parameters in simulation. The investigations of constitutive parametric identification for material dynamic mechanism are mainly from two aspects, one is a constitutive model based on physical microstructures and the other is based on empirical phenomenological. The empirical phenomenological constitutive model is widely used as its intuitive and easy identification of material parameters [11]. Necmi Dusunceli et al. [12] carried on an experiment about creep and relaxation behavior of HDPE under loading-unloading, and determined constitutive parameters for viscoplastic materials using genetic algorithm. Yong Zhang et al.[13] utilized successive artificial neural network technique and particle swarm optimization algorithm to predict Deshpande and Fleck model parameters for aluminum foam at high strain rate. M. Anghileri et al. [14] identified model parameters determining damage and failure mechanisms in fibre-composite materials using an inverse technique based on multi-objective optimization. M.Sedighi et al. [15] identified constitutive model parameters of steel 1018 and 4340 at high strain rate using Hopkinson pressure bar test. For the research of AZ31B magnesium alloy materials, D. Ghaffari Tari et al. [16] studied constitutive behavior of AZ31B considering elevated temperature and anisotropy of tensile-compression, and simulated warm forming process. N Peixinho and A C M Pinho [17] presented results concerning the stiffness and denting

resistance of 6111-T4 aluminum alloy and AZ31B-H24 magnesium alloy, but there was no data related to AZ31B-H24 magnesium alloy dynamic mechanism response. The 6111-T4 aluminum alloy constitutive model was fit to C-S. So far, little research provides dynamic constitutive, strain hardening, rate dependence and energy absorption for the lightest and potential metallic materials magnesium alloys. Only that Fei Feng et al. [18] established AZ31B constitutive considering strain rate using SHTB and fracture model in tensile state; I.R. Ahmad et al. [19] identified AZ31B constitutive parameters considering strain rate using SHPB. The advantage is study for anisotropy and SEM analysis in [19]. Although many investigators mention the potential of magnesium alloys for automotive and aerospace industries, there is no current research related to high strain rate beyond 3000 s^{-1} to 7000 s^{-1} and the structural simulation use of automotive crashworthiness after AZ31B magnesium alloys constitutive parameters identified, which are necessary for automotive transient collision simulation.

In present work, the constitutive parameters of AZ31B-H24 magnesium alloy are identified using SHPB test to fit J-C constitutive model by genetic algorithm. Constitutive parameters are identified by curve fitting over a wide range of strain rate form quasi-static (about 2.1×10-3 s^{-1}) to high dynamic (about 7296 s^{-1}). Constitutive model after parameters identified is applied to automotive outer panels for crashworthiness simulation. In section 2, unknown parameters are defined in J-C constitutive relation. In section 3, the quasi-static test and the SHPB dynamic test are carried on. In section 4, fit the constitutive parameters. In section 5, apply constitutive model to study automotive crashworthiness and conclusions in section 6.

2 Constitutive model

Obviously, nonlinear processes in engineering such as collision, impact and forming process et al. belong to high strain rate problem. The material mechanism characteristics under high strain rate and quasi-static are different [15]. The mechanism characteristics of materials need to be expressed by constitutive equations. J-C mode [20-22] is common used constitutive equation which is belonged to empirical phenomenological constitutive models based on macro-measurable experimental data. The constitutive model is mainly used for materials dynamic plastic relations, which comprehensive reflect metallic constitutive relationship under loadings of large strain, high strain rate and temperature sensitive. The constitutive model has achieved great applications in actual engineering.

After observing material performances at different strains, strain rates and temperatures, Johnson and Cook [21, 22] established an original model J-C to reveal the relationship of flow stress and strain, strain rate and temperature. J-C model is a power-exponent-hardening function. In this equation, Von Mises flow stress is a multiplication form of strain hardening, strain rate dependent and thermal softening.

$$\sigma = \left[A + B\varepsilon_p^N\right]\left[1 + C\ln\left(\frac{\dot{\varepsilon}}{\dot{\varepsilon}_0}\right)\right]\left[1 - \left(\frac{T_i - T_0}{T_m - T_0}\right)^M\right] \quad (1)$$

where σ is Von Mises flow stress, A is yield stress at the reference temperature and reference strain rate, B is the coefficient of strain hardening, N is strain hardening exponent, ε_p is equivalent plastic strain and $\varepsilon_p = \varepsilon - \frac{\sigma}{E}$, E is material elastic modulus, C is the sensitive coefficient of strain rate, M is thermal softening exponent, $\dot{\varepsilon}_0$ is the reference strain rate, $\dot{\varepsilon}$ is the real strain rate, T_i is the test temperature, T_0 and T_m are the reference temperature and the melting temperature, respectively.

In Eq.(1), A, B, C, N, M are the material parametric constants needed to be identified, among A, B, N are obtained by quasi-static tension-compression test, C is by dynamic response and M is by heat resource temperature test. The process such as transit automotive collision in the engineering field is always finished in hundreds milliseconds, so we don't consider the influence of temperature, and the constitutive equation is simplified to Eq.(2).

$$\sigma = \left[A + B\varepsilon_p^N\right]\left[1 + C\ln\left(\frac{\dot{\varepsilon}}{\dot{\varepsilon}_0}\right)\right] \quad (2)$$

3 Quasi-static and dynamic response test

In order to realize structural use, the tests of quasi-static and dynamic over a wide range of strain rates are carried out to identify constitutive parameters and then to develop the proper numerical modeling under nonlinear dynamic mechanism for AZ31B-H24 magnesium alloy. The AZ31B-H24 magnesium alloy materials in this work are from a commercial magnesium alloy company of China. The chemical compositions are illustrated in Tab.1.

Table 1. Chemical composition of AZ31B-H24

elements	Al	Zn	Mn	Si	Fe	Cu	Ni	Ca	Mg
wt.%	2.87	1.0	0.27	< 0.08	< 0.0018	< 0.01	< 0.001	< 0.04	Bal.

3.1 Quasi-static test and results

The quasi-static test is performed on material universal testing machine of SANS (now it is merged by MTS from USA) in Mechanics Experiment Center of South China University of Technology at room temperature. AZ31B-H24 magnesium alloy materials are of anisotropy[23-25], so in present study we carry out tensile and compressive tests under quasi-static.

Specimens for quasi-static tensile test are manufactured by ASTM E8/E8M-15a[26], specimens diagram is shown in Fig.1. In order to eliminate accidental error, 6 group tests are carried out for the same tensile specimens. The average test strain rate is $7\times10^{-4}s^{-1}$. The average true stress versus strain result of quasi-static

tensile test is illustrated in Fig.2(a). AZ31B-H24 magnesium alloy is of no obvious yield step material and the $R_p0.2$ presents its yield strength. The $R_p0.2$ is 147.54 N/mm^2, the tensile strength is 194.63 N/mm^2, and the elongation percentage is 1.25%. Specimens elastic modulus is 45.0GPa.

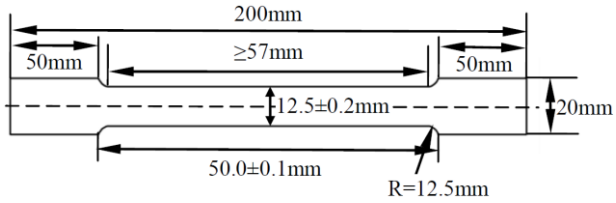

Figure 1. Specimens diagram.

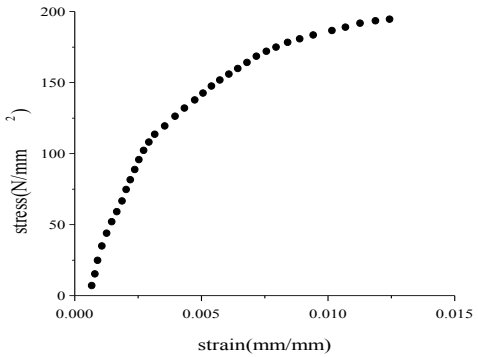

(a) quasi-static tensile

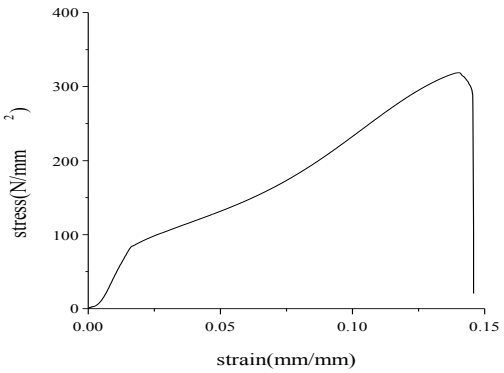

(b) quasi-static compression

Figure 2. Results of quasi-static tensile and compression test for AZ31B-H24.

Specimens for quasi-static compression test are manufactured by ASTM E9-89a (Reapproved 2000)[27], the size for quasi-static compression test is Φ13×25, 4 specimens are used to compression experiment. The average test strain rate is 2.1×10^{-3}s^{-1}, which is reference compression strain rate $\dot{\varepsilon}_0$ in Eq.(2). The average true stress versus strain results of quasi-static compression test is illustrated in Fig.2(b). The peak compressive strength (PCS) in quasi-static compression is 318.76 N/mm^2 and the elongation percentage is 14.56%.

3.2 Dynamic test and results

3.2.1 The SHPB apparatus.

The SHPB test is a widely used and typical technical for identifying material dynamic compression response constants under strain rates 10^2~10^4s^{-1} [28]. The SHPB apparatus is comprised of accelerating chamber, strike bar, incident bar, transmission bar and energy absorption device. The apparatus is shown in Fig.3. The test is carried on in Materials Laboratory of Beijing Institute of Technology. The strike bar is accelerated in helium accelerating chamber, and impact the incident bar. A rectangular elastic pulse is produced in incident bar and spread to specimens to put a dynamic loading. The wave impedances are difference in specimens and incident-transmission bar, a part of incident wave reflects back to incident bar, and the other part enters to transmission bar through specimens. Strain gauges are stuck to incident and transmission bars to measure incident, reflect and transmitted stress wave. Ultra-dynamic strain gauge connected to strain gauge is used to get pulse signal. The stress versus strain relationships are obtained through pulse signal according to one-dimensional stress wave theory.

Figure 3. the SHPB apparatus.

3.2.2 One-dimensional stress wave.

Using the SHPB test to measure material dynamic response for AZ31B-H24 magnesium alloys under high strain rate is based on two assumptions, one is one-dimensional assumption and the other is uniform assumption. According to the two assumptions, one-dimensional stress wave theory can be directly used to determine strain rate $\dot{\varepsilon}(t)$, strain $\varepsilon(t)$, and stress $\sigma(t)$ of materials. The principle diagram of measuring is shown in Fig.4.

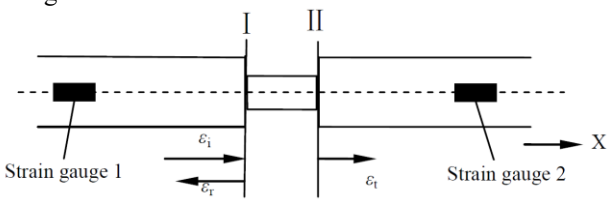

Figure 4. The principle diagram of measuring.

From strain gauge 1 and 2, the incident pulse ε_i, reflect pulse ε_r, and transmission pulse ε_t are obtained. Eq.(3) is the displacement equation according to one-dimensional elastic wave propagation theory.

$$u = C_0 \int_0^t \varepsilon dt \tag{3}$$

Where u is displacement in time t, C_0 is velocity of elastic longitudinal wave, ε is material strain.

In interface I of incident bar and specimens, there are incident strain pulse ε_i in X positive direction and reflect pulse ε_r in X negative direction. The displacement in I is recorded as u_{I},

$$u_{\mathrm{I}} = C_0 \int_0^t (\varepsilon_i - \varepsilon_r) dt \tag{4}$$

Similarly, the displacement u_{II} in interface II is a result by transmission pulse ε_t,

$$u_{\mathrm{II}} = C_0 \int_0^t \varepsilon_t \, dt \tag{5}$$

The average strain $\varepsilon(t)$ in specimens is as follow, l_0 in Eq.(6) is initial length of specimens.

$$\varepsilon(t) = \frac{u_{\mathrm{I}} - u_{\mathrm{II}}}{l_0} = \frac{C_0}{l_0} \int_0^t (\varepsilon_i - \varepsilon_r - \varepsilon_t) dt \tag{6}$$

According to uniform assumption,

$$\varepsilon_r = \varepsilon_t - \varepsilon_i \tag{7}$$

Substitute (7) to (6),

$$\varepsilon(t) = -\frac{2C}{l_0} \int_0^t \varepsilon_r dt \tag{8}$$

$$\dot{\varepsilon}(t) = \frac{2C}{l_0} \varepsilon_r \tag{9}$$

The loadings at both ends of the specimen are F_{I} and F_{II},

$$F_{\mathrm{I}} = EA(\varepsilon_{\mathrm{i}} + \varepsilon_{\mathrm{r}}) \quad F_{\mathrm{II}} = EA\varepsilon_{\mathrm{t}} \tag{10}$$

E is elastic modulus of incident and transmission bars, A is sectional area of bars.

The average stress $\sigma(t)$ can be calculated by Eq.(11),

$$\sigma(t) = \frac{F_{\mathrm{I}} + F_{\mathrm{II}}}{2A_0} = \frac{1}{2} E \left(\frac{A}{A_0} \right) (\varepsilon_i + \varepsilon_r + \varepsilon_t) = E \left(\frac{A}{A_0} \right) \varepsilon_t \tag{11}$$

In Eq.(11), A_0 is specimens section area.

3.2.3 Dynamic response results

In order to study the dynamic mechanism over a wide range of strain rate, the dynamic test is performed on SHPB apparatus in Beijing Institute of Technology. Specimens size is Φ5×5. Specimens of AZ31B-H24 are tested at various strain rates (1389s^{-1}, 2475s^{-1}, 3044s^{-1}, 3801s^{-1}, 4019s^{-1} and 7296s^{-1}). To ensure the repeatability, 3-5 tests are performed for each strain rate. The strain corresponding to PCS and energy absorbing in dynamic compression state are taken up to PCS as in [19]. Results of high strain rates tests dealing with 3.2.2 are illustrated in Fig.5.

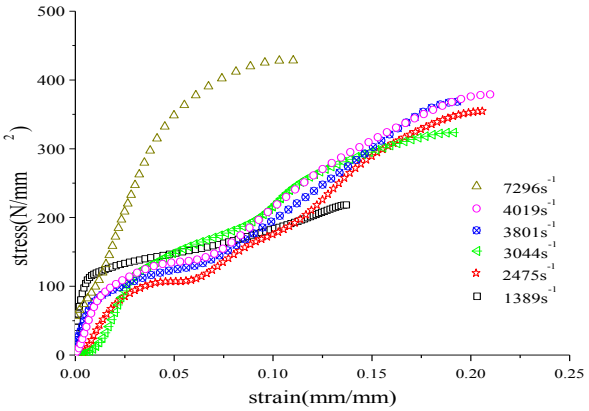

Figure 5. Results of dynamic test.

AZ31B magnesium alloy is a strain-rate-dependent material as described in reference [23-25]. To illustrate the strain rate dependence of the AZ31B-H24 magnesium alloy mechanism at nonlinear stage, the relationship of equivalent plastic strain versus stress is utilized to detailed describe the dynamic response and energy absorption. The first portion of the various strain rates curves is elastic phase, which is linear and of non energy absorption, so it is removed and the rest portion is shown in Fig.6. From Fig.6 we can clearly obtain the strain-rate-dependent characteristic and energy absorption at nonlinear stage. The stress in single strain rate is increasing with increasing equivalent plastic strain. The stress and the initial stress of plastic stage are also increasing with increasing strain rate. The PCS increased with increasing strain rate, however a slight decrease at 3044s^{-1}, the regularity is also obtained in ref [19]. PCS are 218.24MPa, 354.72MPa, 323.54MPa, 368.51MPa, 379.04MPa and 428.40MPa corresponding to 1389s^{-1}, 2475s^{-1}, 3044s^{-1}, 3801s^{-1}, 4019s^{-1} and 7296s^{-1}. The equivalent plastic strain corresponding to PCS is increased at first and then decreased at high strain rate 7296s^{-1} after 4019s^{-1}. The value of initial stress of plastic stage (ISPS), PCS and equivalent plastic strain (EQPS) corresponding to PCS at various experimental strain rates are illustrated in Tab.2.

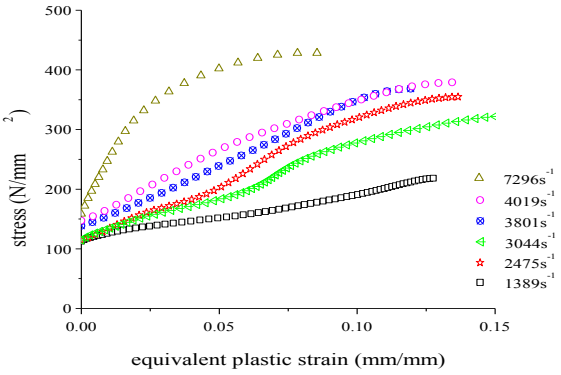

Figure 6. Relationship of equivalent plastic strain versus stress.

Table 2. Detailed value at various strain rates

strain rates(s^{-1})	1389	2475	3044	3801	4019	7296
ISPS (MPa)	112.75	114.50	114.87	138.71	147.30	158.82
PCS(MPa)	218.24	354.72	323.54	368.51	379.04	428.40
EQPS corresponding to PCS(%)	12.76	13.66	15.71	11.94	13.44	8.5

4 Parameters identification

Genetic algorithm (GA) available in Matlab is used to identify parameters in the constitutive equation to meet the results of quasi-static and dynamic mechanism. Evaluation criteria of GA in present work is defined function $f(x)$, minimum of $f(x)$ is the most suitable parameters value.

$$f(x)=\sqrt{\frac{1}{n}\sum_{i=1}^{n}(x-x_i)^2} \tag{12}$$

Where, n is experimental sampling point number, x_i is experimental sampling point value and x is the value of J-C equation with parameters identification.

From the data of Fig.2(b), using GA, we can fit that in J-C Eq.(2) A is 91.487 MPa, B is 4353.112 and N is 1.353. From the data of Fig.6, using GA, we can fit that in J-C Eq.(2) C is 0.033. The contrasts of experimental data versus J-C fit curve are illustrated in Fig.7. The stress versus equivalent plastic strain results of quasi-static compression test is illustrated in Fig.7(a) and high strain rate dynamic compression test is illustrated in Fig.7(b). From Fig.7(a), we can see that the J-C fit curve is completely agreement with the experimental data, and from Fig.7(b) the J-C fit curve is in reasonable agreement with the experimental data except in the last portion of the flow stress curve.

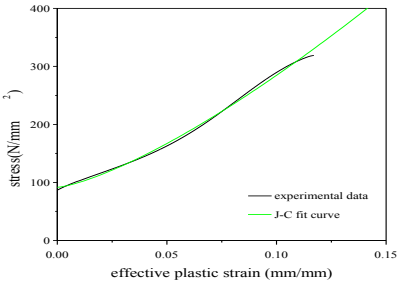

(a) quasi-static compression

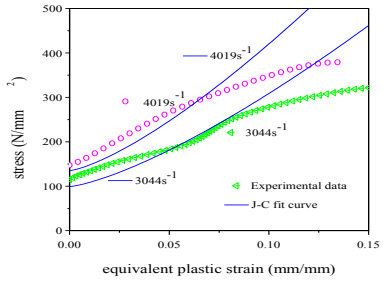

(b) high strain rates dynamic compression

Figure 7. The contrasts of experimental data versus J-C fit curve.

5 Structural panel use simulation

For the use of lightweight magnesium alloy panels into automotive industry, until now only Andrew Parrish, Masoud Rais-Rohani and Ali Najafi [1,8] have replaced the baseline steel parts and performed optimization on the full-scale Dodge Neon model on crashworthiness characteristics. But there is no refer to material mechanism of magnesium alloys, especially dynamic mechanism for nonlinear characteristics such as in this crashworthiness. In present research, identification constitutive parameters are utilized to establish automotive outer panels simulation model for crashworthiness investigation. The contrasts of energy-absorption between AZ31B-H24 magnesium alloy model with J-C constitutive equation and origin steel model are carried on at the premise of 51.18% lightweight.

A full-scale model validated in some automotive group of China is used to compare the energy absorption characteristics of substituting baseline steel with AZ31B-H24 magnesium alloy in current study. A frontal crashworthiness model has been established with Ls-DYNA software, which is shown in Fig.8. Finite element model mass of the whole automotive is 1.588t. The boundary conditions are defined as that initial velocity is 50km/h in the negative direction of X axis, the contact is automatic surface to surface, the friction coefficient between rigid wall and the whole car is 0.3, and the friction coefficient between rigid ground wall and the whole car is 0.7. The AZ31B-H24 magnesium alloy frontal crashworthiness model is established only substitution materials of some panels. The selected automotive panels are illustrated in Fig.9. The change of mass and panel thickness of all selected panels are in Tab.3. The solver time is set as 100ms. Energy curves are calculated and shown in Fig10.

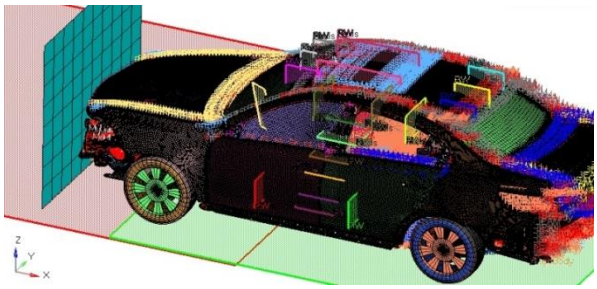

Figure 8. Frontal crashworthiness model

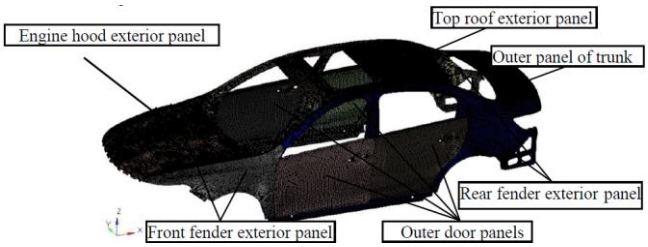

Figure 9. Selected automotive panels

Table 3. The change of materials

automotive parts name	panel thickness(mm)	mass(kg)

	origin model	AZ31B-H24 model	origin model	Z31B-H24 model
engine hood exterior panel	0.7	1.5	8.047	3.932
top roof exterior panel	0.8	1.7	8.767	4.248
outer panel of trunk	0.7	1.5	3.820	1.866
outer door panels	0.7	1.5	15.980	7.806
front fender exterior panel	0.7	1.5	6.497	3.175
rear fender exterior panel	0.7	1.5	23.710	11.59

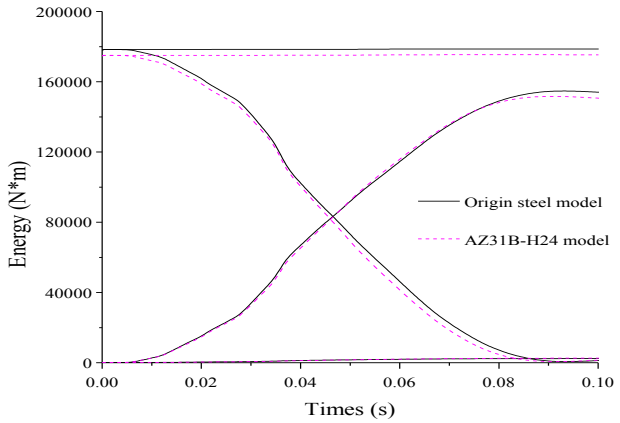

Figure 10. Contrasts of energy-absorption.

Fig.9 shows the automotive panels which we select for structural use investigation. These panels are faced with transient collision and forming impact process. Fig.10 shows the situation of structural energy-absorption, the top of all four curves is total energy, the bottom is hourglass energy, the gradual decline is kinetic energy and the gradual increase is internal energy. Internal energy represents energy absorption capability of component. The mass of selected panels in origin model is 66.82Kg and the energy-absorption is 152.33KJ, while the mass of selected panels in AZ31B-H24 magnesium alloy model is 32.62Kg and the energy-absorption is 149.25KJ. The structural use of AZ31B-H24 magnesium alloy substation of steel can reach 51.18% lightweight and the energy-absorption almost invariable (about 2.0% decrease).

6 Conclusions

The present investigation has provided experimental data for AZ31B-H24 magnesium alloy under quasi-static and high strain rate dynamic situations. In quasi-static mechanism, the material tensile strength is 194.63 N/mm^2 and the elongation percentage is 1.25%, the material compression strength is 318.76 N/mm^2 and the elongation percentage is 14.56%, which reveal anisotropy. In dynamic mechanism, the SHPB test is used to obtain the high strain rate between 1389s^{-1}~7296s^{-1}, which reveal strain-rate-dependent.

Genetic algorithm in Matlab is used to fit J-C constitutive equation. A is 91.487 MPa, B is 4353.112, N is 1.353 and C is 0.033. The J-C fit curve is reasonable agreement with experimental data. These identification parameters are utilized to structural panel use, The selected automotive panels of AZ31B-H24 magnesium alloy substation of steel can reach 51.18% lightweight and the energy-absorption almost invariable.

Acknowledgments

This work is supported by Science&Technology Planning Project of Guangdong Province China (2015B010137002;2016A050503021;2016B090918089) and the Knowledge Innovation Program for Basic Research of Shenzhen City (Fund No. JCYJ20160520164316902).

References

1. Andrew Parrish, Masoud RaisRohani, Ali Najafi, Int. J. Crashworthiness, **17**(3) (2012) 259-281.
2. Pollock TM, Science, **328**(5981) (2010) 986-987.
3. Murray J, King D, Nature, **481**(7382) (2012) 433.
4. W Altenhof, A Raczy, M Laframboise, et al., Int. J. Impact Eng., **30**(2) (2004) 117-142.
5. Xiaoming Chen, Shen-Rong Wu, David A Wagner, et al., Int. J. Crashworthiness, **7**(4) (2002) 429-440.
6. Dørum C, Hopperstad O S, Langseth M, et al., SAE Technical Paper, 2005-01-0724, 2005.
7. Dørum C, Hopperstad O S, Lademo O G, et al., Comput. Struct., **85**(1) (2007) 89-101.
8. A Parrish, M RaisRohani, A Najafi, //52nd AIAA/ASME/ASCE/AHS/ASC Structures, Structural Dynamics and Materials Conference
 19th, 4-7 April 2011, Denver, Colorado.
9. Feng Zhu, Clifford C. Chou, King H. Yang, et al., Int. J. Crashworthiness, **17**(5) (2012) 540-552.
10. DH Liu, HP Yu, CF Li, Mater. Sci. Eng. A, **551** (2012) 280-287.
11. Y Tian, L Huang, H Ma, et al., Mater. Design(1980-2015), **54** (2014) 587-597.
12. N Dusunceli, OU Colak, C Filiz, Mater. Design, **31**(3) (2010) 1250-1255.
13. Y Zhang, G Sun, X Xu, et al., Comp. Mater. Sci., **74** (2013) 65-74.
14. M Anghileri, EC Chirwa, L Lanzi, et al., Compos. Struct., **68**(1) (2005) 65-74.
15. M Sedighi, M Khandaei, H Shokrollahi, Mater. Sci. Eng. A, **527**(15) (2010) 3521-3528.
16. DG Tari, MJ Worswick, J. Mater. Process Tech., **221** (2015) 40-55.
17. N Peixinho, ACM Pinho, P. I. Mech. Eng. D- J. Aut., **220**(9) (2006) 1191-1198.
18. F Feng, S Huang, Z Meng, et al., Mater. Sci. Eng. A, **594** (2014) 334-343.
19. J Xiao, D W Shu, Met. Mater. Int., **21**(5) (2015) 832-831.
20. Johnson G R, Cook W H, *A constitutive model and data for metals subjected to large strains, high strain rates and high temperature* (The Netherlands Publishers, Hague: 1983: 541-547).
21. Johnson GR, Cook WH, Eng. Fract. Mech., **21**(1) (1985) 31-48.
22. G. R. Johnson, W. H. Cook, //Proceeding of 7th International Symposium on Ballistics. The Hague, **21**(1983):541-547.

23. M. T. Tucker, M. F. Horstemeyer, P. M. Gullett, et al., Scr. Metall., **60**(3) (2009) 182-185.
24. G. Wan, B. L. Wu, Y. D. Zhang, et al., Mat. Sci. Eng. A, **527**(12) (2010) 2915-2924.
25. I. R. Ahmad, D. W. Shu, //Applied Mechanics and Materials. Trans Tech Publications, 2012, 151: 726-730.
26. Standard Test Methods for Tension Testing of Metallic Materials.
27. Standard Test Methods of Compression Testing of Metallic Materials at Room Temperature.
28. W. N. Sharpe Jr., *Springer Handbook of Experimental Solid Mechanics*(Springer, 2008).